Systematic error suppression scheme of the weak equivalence principle test by dual atom interferometers in space based on spectral correlation*

Jian-Gong Hu(胡建功)[1,†], Xi Chen(陈曦)[2,3], Li-Yong Wang(王立勇)[4,5], Qing-Hong Liao(廖庆洪)[1], and Qing-Nian Wang(汪庆年)[1]

[1] School of Information Engineering, Nanchang University, Nanchang 330031, China
[2] State Key Laboratory of Magnetic Resonance and Atomic and Molecular Physics, Wuhan Institute of Physics and Mathematics, Wuhan 430071, China
[3] Center for Cold Atom Physics, Chinese Academy of Sciences, Wuhan 430071, China
[4] Center for Optics Research and Engineering, Shandong University, Qingdao 266237, China
[5] School of Information Science and Engineering, Shandong University, Qingdao 266237, China

(Received 14 May 2020; revised manuscript received 29 June 2020; accepted manuscript online 15 July 2020)

Systematic error suppression and test data processing are very important in improving the accuracy and sensitivity of the atom interferometer (AI)-based weak-equivalence-principle (WEP) test in space. Here we present a spectrum correlation method to investigate the test data of the AI-based WEP test in space by analyzing the characteristics of systematic errors and noises. The power spectrum of the Eötvös coefficient η, systematic errors, and noises in AI-based WEP test in space are analyzed and calculated in detail. By using the method, the WEP violation signal is modulated from direct current (DC) frequency band to alternating current (AC) frequency band. We find that the signal can be effectively extracted and the influence of systematic errors can be greatly suppressed by analyzing the power spectrum of the test data when the spacecraft is in an inertial pointing mode. Furthermore, the relation between the Eötvös coefficient η and the number of measurements is obtained under certain simulated parameters. This method will be useful for both isotopic and nonisotopic AI-based WEP tests in space.

Keywords: atom interferometer, weak equivalence principle, spectral correlation, systematic error

PACS: 03.75.Dg, 04.20.Cv, 06.30.Gv, 07.05.Kf **DOI:** 10.1088/1674-1056/aba609

1. Introduction

Atom interferometer (AI) is an important tool with ultra-high precision in acceleration and rotation measurements. Now it has been widely used in many fields[1–3] such as measurements of the gravitational acceleration,[4–10] gravity gradients,[11–14] rotations,[15–18] Newtonian gravitational constant,[19,20] fine structure constant,[21–23] gravitational redshift,[24] post-Newtonian gravity,[25] and so on. Especially, one can perform the test of the weak-equivalence-principle (WEP)[26–33] by measuring the gravity acceleration of two different kinds of atoms. Through sharing a common reflection Raman mirror as well as cooling and manipulating the dual-species atoms synchronously, usually, many noises and systematic errors such as gravity gradients, vibrations and rotations[34,35] can be eliminated. At the same time, errors caused by Zeeman shift and AC-Stark shift can be eliminated by designing AIs with the same internal state in the double Raman transition and Bragg transition interference schemes.[36,37] Therefore, the expected precision of the WEP test could be much higher than the gravity measurement precision.

On this basis, more and more groups in the world are carrying out the AI-based WEP test experiments. Their chosen atoms pairs include isotope atoms, non-isotope atoms, and the same kind of atoms with different spins, and their test accuracy range from 10^{-7} to 10^{-9}.[31,35,38–40] For Mach–Zehnder-type AI-based WEP tests, the measurement sensitivity is inversely proportional to the square of the free evolution time of atoms, thus extending the evolution time is an effective way to improve the test precision. Kasevich's group in Stanford,[38] Zhan's group in WIPM,[39] Rasel's group in Hannover,[40] *etc*., have built long-baseline atomic fountain instruments respectively to extend the free evolution time.

On the other side, the microgravity environment in space provides a nearly ideal platform for atom interferometry. It is possible to further extend the free evolution time, and to prepare atom clouds with lower temperature and better overlaps in space. Moreover, the absence of the large static gravitational force in space also minimizes the necessary lengths for the atom trajectories, therefore, it greatly simplifies and enhances the environmental isolation and controlling of AIs. In addition, the pointing mode of the spacecraft orbit also has an im-

*Project supported by the National Natural Science Foundation of China (Grants No. 11947057), the Foundation for Distinguished Young Scientist of Jiangxi Province, China (Grant No. 2016BCB23009), and the Postdoctoral Applied Research Program of Qingdao City, Shandong Province, China (Grant No. 62350079311135).

†Corresponding author. E-mail: jghu@ncu.edu.cn

© 2020 Chinese Physical Society and IOP Publishing Ltd

portant effect on the precision of AI-based WEP tests in space. The inertial pointing mode has more advantages than the earth-pointing mode. For instance, the errors of AIs are related to the rotation rate of the spacecraft. The smaller the rotation rate is, the smaller the measurement error is. The rotation rate of the spacecraft is zero in the inertial pointing mode. In contrast, the angle between sensitive axes of AIs and earth's gravity varies evenly with the orbital period of the spacecraft. Now several space AI-based WEP projects have been proposed and prepared on the way, and the higher test precision compared with the AI-based WEP on earth is expected to be achieved.[35,41] However, even if the WEP test is violated in space, some systematic errors (for instance, magnetic field, light field distribution, wave-front-aberration, *etc*.) which do not diminish with test sites,[35,41] would be a fatal factor to the improvement of measurement precision since the violation signal will be completely submerged in these errors, and it becomes very difficult to extract signal directly in ultra-high precision tests. Fortunately, the phase difference caused by the violation signal between the interference fringes oscillates sinusoidally in every orbital periods. This gives us a way to extract the violation signal from the noise background. In addition to using microscopic atoms for WEP tests, the MICROSCOPE space mission aims to test the WEP by using macroscopic test masses, which was launched and injected into a circular orbit of 710-km altitude.[42] The satellite, which moves oppositely to the orbit, spins around the normal to the orbital plane. In the satellite frame, the earth's gravity field rotates at the sum of the orbital and spin frequencies. A WEP violation would give a signal modulated at this frequency. However, adding spin frequency only changes the position of signal frequency on the power spectrum, and it does not increase the power spectrum density of the signal.

In this paper, we present a spectral correlation method to effectively analyze and extract the experimental data from the mixed background noises in the AI-based WEP tests in space when the spacecraft is in an inertial pointing mode. By using the method, the WEP violation signal is modulated from DC frequency band to AC frequency band. Our method can effectively suppress the influence of time-independent systematic errors and other errors at the non-sensitive frequency band.

2. AI-based WEP tests in space

2.1. Orbit of the spacecraft

Suppose the orbit of the spacecraft is an ideal roundness. The orientation of the AI sensitive axis along the orbit of the spacecraft is shown in Fig. 1. The spacecraft moves around the earth in inertial pointing mode.

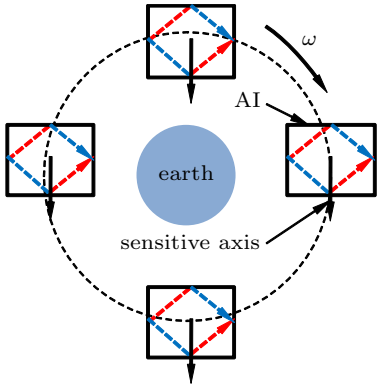


Fig. 1. The schematic diagram of the spacecraft's orbit in space. The spacecraft moves around the earth in inertial pointing mode.

2.2. Systematic errors in AI-based WEP tests

The interferometer is implemented by performing double diffraction beam splitters in a Mach–Zehnder-like $\pi/2$–π–$\pi/2$ configuration. In the AI-based WEP test experiments, by synchronously measuring the accelerations a_j $(j=1,2)$ of two-species atoms (such as ^{85}Rb and ^{87}Rb atoms) and calculating the corresponding differential acceleration ($\Delta a = a_2 - a_1$) to the projection of local g in direction of the sensitive axis, we can get the Eötvös coefficient η of the WEP which can usually be described as

$$\eta = \frac{a_2 - a_1}{g}. \tag{1}$$

The AIs' phase is influenced by variations of the environmental parameters such as gravity, gravity gradients, rotations, magnetic field, vibrations, wave-front-aberration,[43] and so on. We assume that $k_{\mathrm{eff},1}$ and $k_{\mathrm{eff},2}$ are the effective wave vectors of the dual-species AIs. $\alpha = k_{\mathrm{eff},2}/k_{\mathrm{eff},1}$ is the ratio between the two wave vectors. After Nnumber of measurements, the populations for different internal spin states of two AIs are[44]

$$\begin{cases} P_1[i] = \dfrac{1}{2}\left[1+\cos(k_{\mathrm{eff},1}a_1T^2 + \phi_{d,1}[i] + \phi_{\mathrm{scan},1}[i])\right], \\ P_2[i] = \dfrac{1}{2}\left[1+\cos(k_{\mathrm{eff},2}a_2T^2 + \phi_{d,2}[i] + \phi_{\mathrm{scan},2}[i])\right], \end{cases} \quad i = 1,2,\ldots,N, \tag{2}$$

where i means the number of interference. $\phi_{a,j} = k_{\mathrm{eff},j}a_jT^2$ $(j=1,2)$ are acceleration-induced phases of these two AIs. T is the free evolution time. We have introduced scanning phases $\phi_{\mathrm{scan},j}[i]$ $(j=1,2)$ which changes at every measurement data point and is used to change the total phases to form the sine curves or an ellipse curve. The environment back-

ground induced phases are defined as $\phi_{d,j}[i]$ $(j=1,2)$ at each interference period.

By synchronously scanning the phase ($\phi_{\text{scan}}[i] = \phi_{\text{scan},1}[i] = \phi_{\text{scan},2}[i]$) and parametrically plotting P_1 *versus* P_2, an elliptic curve is obtained as shown in Fig. 2(a). The shape of the ellipse curve represents the phase differences between these two AIs, and the information of Eötvös coefficient η is derived by fitting the differential phase of this elliptic curve. However, for nonisotopic dual-AI experiments, the $k_{\text{eff},1}$ and $k_{\text{eff},2}$ are different, their difference gives a phase shift $\Delta k_{\text{eff}} g T^2$.[44] In general, the environment-induced phases $\phi_{d,j}[i]$ $(j=1,2)$ are different so that an additional phase shift is caused.

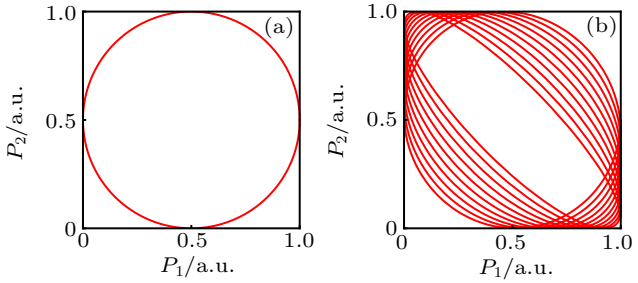


Fig. 2. The elliptic curve and the Lissajous curve. (a) The elliptic curve obtained by synchronously scanning the phase and plotting P_1 *versus* P_2, the range of ϕ_{scan} is 2π. (b) The Lissajous curve obtained by plotting P_1 *versus* P_2. The ratio of effect vectors is α =780/767, and the range of $\phi_{\text{scan},1}$ is 20π.

If the ratio between the environment-induced phase $\phi_{d,2}[i]/\phi_{d,1}[i] = \alpha$, it does not lead to a deviation in the WEP test. We can utilize a proportional-scanning-phase method[44] to suppress the phase shift. For instance, the wave-front-aberration phases and the vibration-induced phases are proportional to the effective wave vectors $k_{\text{eff},j}$,[43,44] and they all have the same ratio. We scan the phases and the effective wave vectors $\phi_{\text{scan},1}[i]/\phi_{\text{scan},2}[i] = \alpha$ with the same ratio and plot P_1 *versus* P_2. A Lissajous curve is obtained as shown in Fig. 2(b). The populations of internal states of two AIs can be written as

$$\begin{cases} P_1[i] = \dfrac{1}{2}\left[1+\cos(\phi_{\text{com}}[i])\right], \\ P_2[i] = \dfrac{1}{2}\left[1+\cos(\alpha\phi_{\text{com}}[i]+\phi_{\text{diff}}[i])\right], \end{cases} \quad i=1,2,\ldots,N, \tag{3}$$

where $\phi_{\text{com}}[i] = k_{\text{eff},1} a_1 T^2 + \phi_{\text{d},1}[i] + \phi_{\text{scan},1}[i]$ is defined as the common-mode phase. $\phi_{\text{diff}}[i] \equiv k_{\text{eff},2}\eta[i] g T^2$ is the residual phase. We define $\phi_{\text{diff}}[i] \equiv k_{\text{eff},2}\eta[i] g T^2$ as the differential-mode phase, and it is also the Eötvös coefficient phase. It can be derived by using the Bayesian estimation method.[45] The information of η can be described as

$$\eta[i] = \frac{\phi_{\text{diff}}[i]}{k_{\text{eff},2} g T^2}. \tag{4}$$

If the ratio of phase $\phi_{d,j}[i]$ $(j=1,2)$ induced by the environment background is not α, the systematic phase of the mean field will be independent from $k_{\text{eff,j}}$.[41] There is a systematic error in WEP tests, it can be described as

$$\Delta\eta[i] = \frac{\phi_{d,2}[i]}{k_{\text{eff},2} g T^2} - \frac{\phi_{d,1}[i]}{k_{\text{eff},1} g T^2}. \tag{5}$$

3. Power spectrum for the violation signal of WEP tests in space

In the inertial pointing mode, the phase difference between the interference fringes caused by the violation signal oscillates sinusoidally with the orbital period. And the phase difference induced by the environment background oscillates sinusoidally with other different periods. Fortunately, the information of η can be derived from the difference of power spectrum between the violation signal and noises. When the spacecraft goes around the earth, the angle θ between the sensitive axis of AI and the earth's gravity varies evenly with the orbital period of the spacecraft. Once the WEP is violated, the differential-mode phase $\phi_{\text{diff}}[i]$ of the interference fringes caused by the violation signal will oscillate sinusoidally with the orbital period. Therefore, the time-domain description of the differential-mode phase can be rewritten as

$$\phi_{\text{diff}}(t) = A\sin(\omega t + \phi_{\text{ini}}), \tag{6}$$

where A is the sinusoidal amplitude, $\theta = \omega t$, ω is the angular frequency of the orbital period of the spacecraft. ϕ_{ini} is the initial phase. Here we set $\phi_{\text{ini}} = 0$ to simplify the calculation. To make a meaningful estimation of the statistical process in the presence of correlations, one has to specify the number of measurements N. A single measurement time (cycle time) is t, and $2T = Nt$ is the total measurement time. Notice that the T in here represents a half of the total measurement time. Hence the autocorrelation function of the differential-mode phase of the violation signal can be defined by[46]

$$R_\phi(m) = \lim_{N\to\infty}\frac{1}{N}\sum_{i=0}^{N-1}\phi_{\text{diff},i}\phi_{\text{diff},i+m}, \tag{7}$$

we transfer Eq. (7) into the frequency domain by using the Fourier transformation. It can be then expressed below:

$$\begin{aligned} R_\phi(m) &= \lim_{N\to\infty}\frac{1}{N}\sum_{i=0}^{N-1}\phi_{\text{diff},i}\phi_{\text{diff},i+m} \\ &= \lim_{N\to\infty}\frac{1}{N}\sum_{i=0}^{N-1}\lim_{N\to\infty}\frac{1}{Nt}\sum_{j=0}^{N-1}F_j\,\mathrm{e}^{-I2\pi ij/N} \\ &\quad\times\lim_{N\to\infty}\frac{1}{Nt}\sum_{j'=0}^{N-1}F_{j'}\,\mathrm{e}^{-I2\pi(i+m)j'/N} \\ &= \lim_{N\to\infty}\frac{1}{N}\lim_{N\to\infty}\frac{1}{Nt}\sum_{j=0}^{N-1}\lim_{N\to\infty}\frac{1}{Nt}\sum_{j'=0}^{N-1} \\ &\quad\times\left(\sum_{i=0}^{N-1}\mathrm{e}^{-I2\pi i(j+j')/N}\right)F_jF_{j'}\,\mathrm{e}^{-I2\pi mj'/N} \end{aligned}$$

$$= \lim_{N\to\infty}\frac{1}{Nt}\sum_{j=0}^{N}\lim_{N\to\infty}\frac{1}{Nt}\sum_{j'=0}^{N-1}\delta_{j'=-j}F_jF_{j'}\,\mathrm{e}^{-I2\pi mj'/N}$$

$$= \lim_{N\to\infty}\frac{1}{N^2t^2}\sum_{j=0}^{N-1}F_jF_{-j}\,\mathrm{e}^{I2\pi mj/N}$$

$$= \lim_{N\to\infty}\frac{1}{Nt}\sum_{j=0}^{N-1}\frac{|F_j|^2}{Nt}\,\mathrm{e}^{I2\pi mj/N}, \tag{8}$$

where $F_j = \sum_{i=0}^{N-1}\phi_{\mathrm{diff},i}\,\mathrm{e}^{I2\pi ij/N}$ is the discrete Fourier transformation of $\phi_{\mathrm{diff},i}$.

$$S_{\phi_{\mathrm{diff}},j} = \lim_{N\to\infty}\frac{|F_j|^2}{Nt}$$

represents the power spectral density of the differential-mode phase fluctuations. Equation (8) can be rewritten as

$$R_\phi(m) = \lim_{N\to\infty}\frac{1}{Nt}\sum_{j=0}^{N-1}S_{\phi_{\mathrm{diff}},j}\,\mathrm{e}^{I2\pi mj/N}. \tag{9}$$

For stationary stochastic processes, the autocorrelation function must be an even function, *i.e.*, $R_\phi(m) = R_\phi(-m)$. The value of the autocorrelation function for $m = 0$ represents the variance of the differential-mode phase fluctuations

$$R(m=0) = \sigma^2_{\phi_{\mathrm{diff}}} = \lim_{N\to\infty}\frac{1}{Nt}\sum_{j=0}^{N-1}S_{\phi_{\mathrm{diff}},j}. \tag{10}$$

If the power spectrum of the differential-mode phase fluctuations comes from white noise, the amplitude of noise power spectrum density (NPSD) $S_\eta(v)$ can be derived as

$$S_\eta(v) = \sigma_\eta\sqrt{t}, \tag{11}$$

where σ_η is the standard deviation of noises in a single measurement cycle. t is the single measurement time. v is the frequency of periodic oscillation. In addition, if the power spectrum of the differential-mode phase fluctuations comes from the systemic errors of DC, the power spectrums of the systematic errors will be in the zero frequency band, which are not in the same frequency band with the WEP violation signal. Similarly, the differential-mode phase of the interference fringe caused by the violation signal will oscillate sinusoidally with the orbital period. Equation (10) can be rewritten as

$$\frac{1}{N}\sum_{i=0}^{N-1}\phi^2_{\mathrm{diff},i} = \frac{1}{Nt}S_{j=v}, \tag{12}$$

where $S_{j=v}$ is the power spectrum density of the violation signal. A power spectrum impulse is generated at frequency v when one performs the WEP test in the spacecraft, the amplitude of this impulse can be expressed as

$$S_{\eta 0} = \frac{1}{2}\eta_0\sqrt{Nt}, \tag{13}$$

where η_0 is the amplitude of the violation signal in the WEP test experiment.

4. Simulation results and discussion

Here, we suppose the altitude of the spacecraft is 1000 km. A single measurement time is $t = 20$ s, and the number of measurements is $N = 10000$. According to the altitude of spacecraft, it is easy to know the orbital period of spacecraft is 6313 s, and the frequency of the WEP breakdown signal of the sinusoidal oscillation is 1/6313 Hz. This frequency is defined as the sensitive frequency.

Figure 3 shows the full power spectrum of the WEP breakdown signal and noises together. The phase ϕ_d caused by environment noises forms the background of the full power spectrum (that is the amplitude of (NPSD) $S_\eta(v)$). In Fig. 3(a), the breakdown signal of WEP is mixed in the background noises. In Figs. 3(b)–3(d), there is a peak signal in the sensitive frequency band (1/6313 Hz). This peak represents the breakdown signal of WEP which is caused by the acceleration-induced phase ϕ_a. The smaller the standard deviation σ_η of the noise is, the more obvious this peak is.

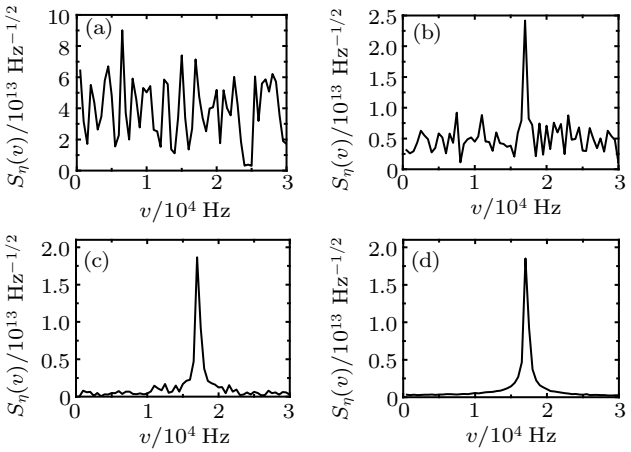


Fig. 3. Numerical simulation of the power spectrum of WEP tests in space. The Eötvös coefficient η_0 is set to be 1×10^{-15}. The standard deviations of noises in a single measurement cycle are set to be (a) 1×10^{-13}, (b) 1×10^{-14}, (c) 1×10^{-15}, and (d) 1×10^{-16}, respectively.

The value of the peak in the sensitive frequency band of Fig. 3(a) cannot be distinguished from the background of the full power spectrum. This is because the number of measurements set here is too little compared to the standard deviation σ_η of the noise. The intensity of the background noise is much bigger than the intensity of the breakdown signal of WEP. This problem can further be overcome by increasing the number of measurements. When the number of measurements is increased to 1×10^6, an obvious peak of the breakdown signal of WEP appears in the sensitive frequency band, as shown in Fig. 4.

To determine whether the WEP breakdown is true, we must make sure that the amplitude of this peak is much bigger than the amplitude of the background noise. When the amplitude of this peak is 5 times bigger than that of the background noise ($S_{\eta 0}/S_\eta(v) > 5$), the probability of the WEP breakdown is 99.99994%. In order to achieve the above probability and

by substituting Eq. (11) into Eq. (13), the number of the WEP measurements should meet the following condition:

$$N > \left(\frac{10\sigma_\eta}{\eta_0}\right)^2. \tag{14}$$

On the contrary, if the peak is not 5 times bigger than the amplitude of the background at the sensitive frequency, the Eötvös coefficient η can be described as

$$\eta_0 < \frac{10\sigma_\eta}{\sqrt{N}}, \tag{15}$$

that is to say, there is no 99.99994% probability that the WEP breakdown will occur. It will occur with a low probability, for example, 90% or lower. η_0 is commonly called the precision of the WEP test.

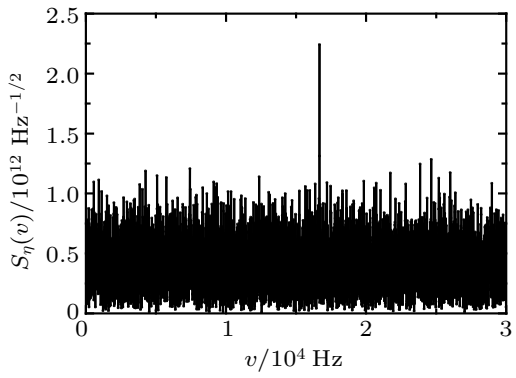


Fig. 4. Numerical simulation of the power spectrum of WEP tests in space. On the basis of Fig. 3(a), the number of measurements is increased to 1×10^6. σ_η is 1×10^{-13}.

By analyzing the power spectrum of the test data, the information of the WEP test signal can be effectively extracted and the influence of systematic errors can be effectively suppressed. For the AI-based WEP tests in space, there are many systematic errors such as vibrations, wave-front-aberration, fixed magnetic field, and light field distributions which do not vary with time. They are defined as the time-independent DC errors in here. Although the intensities of these errors are much greater than the intensity of the breakdown signal of WEP, these errors do not affect the power spectrum of the Eötvös coefficient η. In addition, errors in the non-sensitive frequency band can be effectively eliminated in the power spectrum. For instance, the power spectrum of the phase difference caused by gravity gradients repeats at twice of the period of the Eötvös coefficient η, thus the error caused by gravity gradients can be effectively eliminated.[47] Therefore, power spectrum analysis is very useful for the extraction of test data of the WEP test in space.

5. Conclusion

In summary, the paper presents a spectrum correlation method to investigate the test data of the AI-based WEP tests in space. The power spectrum of the Eötvös coefficient η, systematic errors, and noises in the AI-based WEP tests in space are analyzed and calculated in detail. When the spacecraft is in an inertial pointing mode, we find that the signal can be effectively extracted and the influence of systematic errors can be greatly suppressed by analyzing the power spectrum of the measurement data in the AI-based WEP tests in space. This is a useful way to suppress the systematic errors in AI-based WEP tests in space. Furthermore, the relation between the Eötvös coefficient η and the number of measurements can be obtained under certain simulated parameters. Our scheme will be helpful for the future design of ultra-high-precision AI-based WEP tests in space, and it is suitable for both isotopic and nonisotopic AIs-based WEP tests.

References

[1] Kasevich M and Chu S 1991 *Phys. Rev. Lett.* **67** 181
[2] Cronin A D, Schmiedmayer J and Pritchard D E 2009 *Rev. Mod. Phys.* **81** 1051
[3] Barrett B, Cheiney P, Battelier B, Napolitano F and Bouyer P 2019 *Phys. Rev. Lett.* **122** 043604
[4] Zhou M K, Duan X C, Chen L L, Luo Q, Xu Y Y and Hu Z K 2015 *Chin. Phys. B* **24** 050401
[5] Bidel Y, Carraz O, Charri'ere R, Cadoret M, Zahzam N and Bresson A 2013 *Appl. Phys. Lett.* **102** 144107
[6] Hu Z K, Sun B L, Duan X C, Zhou M K, Chen L L, Zhan S, Zhang Q Z and Luo J 2013 *Phys. Rev. A* **88** 043610
[7] Cheng B, Wang Z Y, Xu A P, Wang Q Y and Lin Q 2015 *Chin. Phys. B* **24** 113704
[8] Karcher R, Imanaliev A, Merlet S and Dos Santos F P 2018 *New J. Phys.* **20** 113041
[9] Fang J, Hu J G, Chen X, Zhu H R, Zhou L, Zhong J Q, Wang J and Zhan M S 2018 *Opt. Express* **26** 1586
[10] Wu B, Cheng B, Fu Z J, Zhu D, Zhou Y, Weng K X, Wang X Long and Lin Q 2018 *Acta Phys. Sin.* **67** 190302 (in Chinese)
[11] Sorrentino F, Bodart Q, Cacciapuoti L, Lien Y H, Prevedelli M, Rosi G, Salvi L and Tino G M 2014 *Phys. Rev. A* **89** 023607
[12] Snadden M J, McGuirk J M, Bouyer P, Haritos K G and Kasevich M A 1998 *Phys. Rev. Lett.* **81** 971
[13] Pereira Dos Santos F 2015 *Phys. Rev. A* **91** 063615
[14] Duan X C, Zhou M K, Mao D K, Yao H B, Deng X B, Luo J and Hu Z K 2014 *Phys. Rev. A* **90** 023617
[15] Guastavson T L, Landragin A and Kasevich M A 2000 *Class. Quantum Gravity* **17** 2385
[16] Yao Z W, Lu S B, Li R B, Wang K, Cao L, Wang J and Zhan M S 2016 *Chin. Phys. Lett.* **33** 083701
[17] Canuel B, Leduc F, Holleville D, Gauguet A, Fils J, Virdis A, Clairon A, Dimarcq N, Bordé Ch J and Landragin A 2006 *Phys. Rev. Lett.* **97** 010402
[18] Savoie D, Altorio M, Fang B, Sidorenkov L A, Geiger R and Landragin A 2018 *Sci. Adv.* **4** eaau7948
[19] Rosi G, Sorrentino F, Cacciapuoti L, Prevedelli M and Tino G M 2014 *Nature* **510** 518
[20] Fixler J B, Foster G T, McGuirk J M and Kasevich M A 2007 *Science* **315** 74
[21] Chiow S W, Herrmann S, Chu S and Müller H 2009 *Phys. Rev. Lett.* **103** 050402
[22] Bouchendira R, Cladé P, Guellati-Khélifa S, Nez F and Biraben F 2011 *Phys. Rev. Lett.* **106** 080801
[23] Parker R H, Yu C H, Zhong W C, Estey B and Muller H 2018 *Science* **360** 191
[24] Müller H, Peters A and Chu S 2010 *Nature* **463** 926
[25] Müller H, Chiow SW, Herrmann S, Chu S and Chung K Y 2008 *Phys. Rev. Lett.* **100** 031101
[26] Zhou L, Long S T, Tang B, Chen X, Gao F, Peng W C, Duan W T, Zhong J Q, Xiong Z Y, Wang J, Zhang Y Z and Zhan M S 2015 *Phys. Rev. Lett.* **115** 013004

[27] Zhou L, He C, Yan S T, Chen X, Duan W T, Xu R D, Zhou C, Ji Y H, Sachin B, Wang Q, Hou Z, Xiong Z Y, Gao D F, Zhang Y Z, Ni W T, Wang J and Zhan M S 2019 arXiv:1904.07096v2 [quant-ph]

[28] Zhan M S, Wang J, Ni W T, *et al*. 2019 *Int. J. Mod. Phys. D* **29** 1940005

[29] Schlippert D, Hartwig J, Albers H, Richardson L L, Schubert C, Roura A, Schleich W P, Ertmer W and Rasel E M 2014 *Phys. Rev. Lett.* **112** 203002

[30] Tarallo M G, Mazzoni T, Poli N, Sutyrin D V, Zhang X and Tino G M 2014 *Phys. Rev. Lett.* **113** 023005

[31] Duan X C, Deng X B, Zhou M K, Zhang K, Xu W J, Xiong F, Xu Y Y, Shao C G, Luo J and Hu Z K 2016 *Phys. Rev. Lett.* **117** 023001

[32] Wang J and Zhan M S 2018 *Acta Phys. Sin.* **67** 160402 (in Chinese)

[33] Deng X B, Duan X C, Mao D K, Zhou M K, Shao C G and Hu Z K 2017 *Chin. Phys. B* **26** 043702

[34] Bonnin A, Zahzam N, Bidel Y and Bresson A 2015 *Phys. Rev. A* **92** 023626

[35] Aguilera D N, Ahlers H, Battelier B, *et al*. 2014 *Class. Quantum Gravity* **31** 115010

[36] Lévèque T, Gauguet A, Michaud F, Pereira F, Dos Santos F P and Landragin A 2009 *Phys. Rev. Lett.* **103** 080405

[37] Giese E, Roura A, Tackmann G, Rasel E M and Schleich W P 2013 *Phys. Rev. A* **88** 053608

[38] Sugarbaker A, Dickerson S M, Hogan J M, Johnson D M S and Kasevich M A 2013 *Phys. Rev. Lett.* **111** 113002

[39] Zhou L, Xiong Z Y, Yang W, Tang B, Peng W C, Hao K, Li R B, Liu M, Wang J and Zhan M S 2011 *Gen. Relat. Gravity* **43** 1931

[40] Hartwig J, Abend S, Schubert C, Schlippert D, Ahlers H, Posso-Trujillo K, Gaaloul N, Ertmer W and Rasel E M 2015 *New J. Phys.* **17** 035011

[41] Williams J, Chiow S W, Yu N and Müller H 2016 *New J. Phys.* **18** 025018

[42] Touboul P, Métris G, Rodrigues M, *et al*. 2017 *Phys. Rev. Lett.* **119** 231101

[43] Hu J G, Chen X, Fang J, Zhou L, Zhong J Q, Wang J and Zhan M S 2017 *Phys. Rev. A* **96** 023618

[44] Chen X, Zhong J Q, Song H W, Zhu L, Wang J and Zhan M S 2014 *Phys. Rev. A* **90** 023609

[45] Stockton J K, Wu X A and Kasevich M A 2007 *Phys. Rev. A* **76** 033613

[46] Fritz R 2004 *Frequency Standards-Basics and Applications* (Germany: Wiley-Vch Verlag) pp. 48–78

[47] Chiow S W, Williams J, Yu N and Müeller H 2017 *Phys. Rev. A* **95** 021603